

UNDERSTANDING MICROWAVE HEATING CAVITIES IN USE TODAY

Per O Risman, Microtrans AB, Landvetter Sweden

A. Cavity volume resonances, matching and coupling factors

A.1 Introduction

Since the upper (ceiling) and lower (bottom) ends of an oven cavity are closed by metal, the load is near the bottom, and the cavity height is comparable to or larger than λ_0 one can analyse the system by assuming that waves propagate upwards and downwards and set up standing wave patterns in the vertical direction in a right-angled rectangular cavity[†]. These patterns are thus in principle determined by the same criteria as those in the horizontal directions. A typical load is essentially a flat horizontal slab and can – for the purpose of this analysis – be approximated by a slab extending to all four vertical cavity walls.

Since the cavity has to be energised and the load is at the bottom, it is suitable to discuss the energy coupling, field amplitudes and resonance phenomena under the assumption that the energy input is at the cavity ceiling. It can be shown that only a small coupling area is needed, so that most of the retro-reflected energy from the slab load is reflected back downwards. In reality, the ceiling area is partially a reflector for the returning wave and partially an aperture that allows power to flow into the cavity and back into the feeding transmission line.

The analytical scenario is illustrated in figure A-1. The stationary input signal C_1^+ into the cavity is normalised to 1, but since the matching conditions at the aperture are not the same at the beginning as under stationary conditions, the cavity input signal with the transmission line signal as reference will gradually approach its stationary value.

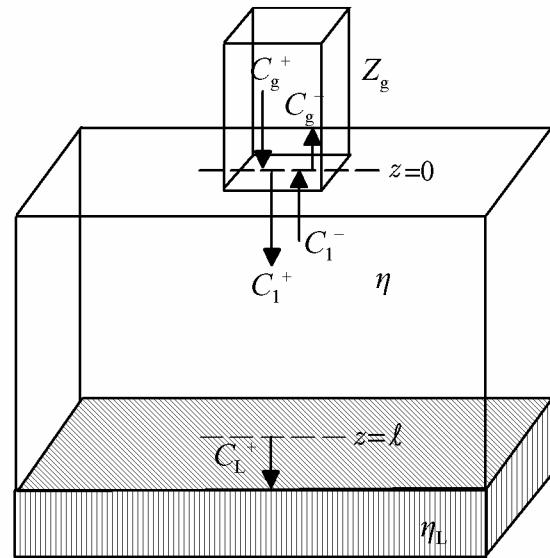


Figure A-1. Cavity feed and stationary signals

A.2 Coupling factor and system matching

The reflection factor r^- is the electric field reflection factor at the load interface, and the minus superscript is for the upwards propagation direction, away from the load. It is determined by the general formula

$$r^- = \frac{\eta_L - \eta}{\eta_L + \eta}$$

(A-1)

[†] The theory here is in principle applicable to all cylindrical cavity geometries, i.e. those having a constant cross section in the z direction. In practise, the circularly cylindrical geometry is the only other which is reasonably easy to use. However, TE and TM modes are not degenerate in the same way for circular cross section, so hybrid mode solutions can normally not be calculated analytically.



where η is the wave impedance of the cavity volume mode under study, and η_L the wave impedance of this mode inside the load. If the load ε is complex, \underline{r}^- also becomes complex. However, the spatial phase of \underline{r}^- due to the distance ℓ between the load and the reference plane at the ceiling and aperture must also be included (as $\exp(-j k \ell)$, where k is the cavity mode wavenumber). As discussed in section 3.3.3, no significant error is introduced by using $|\eta_L|$ instead of η_L , with typical dielectrics such as foods. This means that \underline{r}^- can be considered negative real, r^- , at $z = \ell$.

The cavity is fed by a transmission line, through an aperture (port), and the conditions in this feed plane may conveniently be characterised as in figure A-1. The characteristic impedance of the transmission line between the generator and the cavity is Z_g . The propagating, stationary (time-harmonic) signal amplitudes in the forward and backward directions in the transmission line are C_g^+ and C_g^- . The quotient C_g^-/C_g^+ is the transmission line reflection factor Γ ; it may be expressed as a complex number $|\Gamma|e^{j\phi}$, representing its amplitude and phase angle in a suitable reference plane which may be the cavity port or the generator coupling plane in the transmission line behind. In the cavity space the signals are C_1^+ and C_1^- , respectively. The quotient C_1^-/C_1^+ is the cavity load reflection factor \underline{r}^- , and refers to the reference plane in the cavity ceiling.

It is common not to make sufficient distinction between transmission line and wave propagation quantities in descriptions and analysis of systems of the kind dealt with here. Not only impedance but also field matching are important in the junction between a transmission line and a cavity with a mode. For that reason, different notation is recommended for transmission line impedances and reflection factors (Z and Γ) and for the corresponding wave quantities (η and r). The proper integration is done in the aperture plane. – The boundary conditions for voltage and current in the port plane then give

$$C_g^+(1 + \Gamma) = C_1^+(1 + \underline{r}^-) \quad (\text{voltage and } E \text{ field}) \quad (\text{A-2a})$$

$$C_g^+(1 - \Gamma)/Z_g = C_1^+(1 - \underline{r}^-)/\eta \quad (\text{current and } H \text{ field}) \quad (\text{A-2b})$$

It is convenient to label[†] the quotient

$$Z_g/\eta \equiv \kappa_{g,1} \equiv \kappa \quad (\text{A-3})$$

κ is the *coupling impedance ratio* and is an important parameter in cavity studies.

The aperture reflection factor r^+ as seen from the cavity is thus

$$r^+ = (Z_g - \eta)/(Z_g + \eta) = (\kappa - 1)/(\kappa + 1) \quad (\text{A-4})$$

It is important to note that our κ does not only include an impedance matching or mismatching condition but also a field matching or mismatching: Z_g is a transmission line characteristic impedance, whereas η and also η_L are the characteristic wave impedances of a unidirectionally propagating mode in the cavity and load, respectively. Both Z_g and η_L thus represent specific *modes*.

It is assumed here that Z_g is approximately real, since the cavity is fed directly by a transmission line. Since η is also real, κ is also approximately real. If the cavity is fed by a very small aperture, $Z_g \rightarrow 0$.

Resonance – constructive interference between the upwards and downwards propagating waves – is now assumed. Furthermore, matching of the feed line ($\Gamma = 0$) is assumed. Insertion of equation (A-1) into equations (A-2) and subtracting the latter then gives

$$Z_g = \eta_L \quad \chi = 1 \quad r^+ = r^- = r_R \quad \kappa = \frac{1 + r_R}{1 - r_R} \quad (\text{matching at resonance}) \quad (\text{A-6})$$

[†] This, and the approach used here, does not appear in the literature. The greek letter kappa (κ) has been used by some authors instead of ε for relative permittivity, but the risk of confusion here is minimal.

A.3 Single mode system matching and Γ relationships for varying input

In the scenario in figure A-1, the aperture is supposed to have field matching to only the single mode which is studied. This is theoretically possible if the aperture covers the whole horizontal cross section, since waveguide modes are orthogonal. A way of physically constructing such a feed is to completely fill the feeding waveguide with a dielectric. Its Z_g then becomes $\eta/\sqrt{\epsilon}$. To feed this dielectric-filled waveguide in turn with only the desired mode may pose a still larger problem, but the point of the reasoning is that a cavity with the desired properties may be constructed.

In practise, a smaller aperture is used, without a dielectric. This may then create more than one cavity mode, since it is only partially field matched to the possible modes.

A practical resonant cavity system for heating has to be efficient and must thus be reasonably well matched. κ for the single mode under study may then be set for system matching at resonance ($\chi=1$). The perfectly field matched feed as described above is used in this analysis of single mode behaviour. The frequency dependence of the stationary Γ ($=C_g^-/C_g^+$) can then be used as a practically relevant output variable for determination of frequency bandwidth and other data for example by a standard polar (Smith) chart. κ at resonance (κ_R) is then firstly calculated and Z_g is then considered constant (frequency independent) in the following calculations. Γ is thus set to 0 at resonance (and for unidirectional propagation in the cavity). By solving equations (A-2) for Γ as a function of frequency within a suitable band, one obtains

$$\Gamma = \frac{1 + \underline{r}^- - \kappa_R \cdot (1 - \underline{r}^-)}{1 + \underline{r}^- + \kappa_R \cdot (1 - \underline{r}^-)} \quad (\text{A-7})$$

Note that \underline{r}^- refers to the E_{hor} field at the cavity ceiling and becomes negative real at TE mode resonance. A sign change is made when the calculations use the H_{hor} field as reference; this is the case for TM modes. For these, the sign of \underline{r}^- changes when ν^\dagger passes the Brewster value ν_B ; the modified \underline{r}^- thus becomes +1 for $\nu=1$.

$\nu \cdot f$ is constant (it equals the “cut-off” frequency f_c). ν must thus be varied to maintain constant cavity geometry under frequency change. Of course, the frequency dependence of ν has to be used also in the relationships for k_z and in the recalculations of \underline{r}^- . Insertion of the impedance relationships in Table A-1[†] into the definition of κ gives, with $\epsilon=1$ for the cavity space

$$\kappa^2 = \kappa_R^2 \cdot (1 - \nu^2) / (1 - \nu_R^2) \quad (\text{TEz modes}) \quad (\text{A-8a})$$

$$\kappa^2 = \kappa_R^2 \cdot (1 - \nu_R^2) / (1 - \nu^2) \quad (\text{TMz modes}) \quad (\text{A-8b})$$

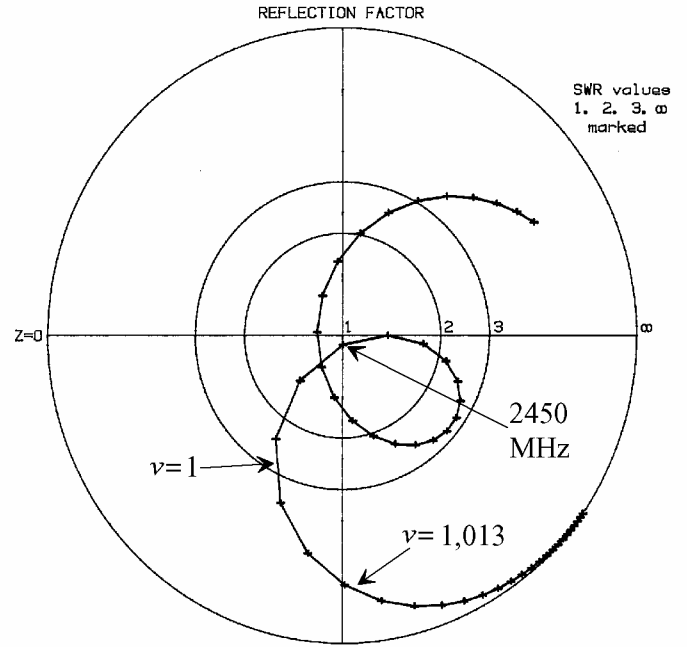


Figure A-2. The system Γ in a microwave oven scenario for one Brewster (TM) mode ($\nu=0,992$) with $\kappa=0,939$ at 2450 MHz. Load $\epsilon=52-j20$. 9,8 MHz between frequency markers; clockwise increase.

[†] See the table in the Appendix. The normalised wavelength ν is f_c/f , where f_c is the mode “cut-off” frequency.



For variable frequency calculations, κ thus replaces κ_r in equation (A-7).

There is a mathematical singularity for $\nu=1$, as r^- becomes exactly -1 irrespective of system dimensions, for both TE and TM (before TM sign reversal). For TM, $\kappa \rightarrow \infty$ at $\nu=1$ for increasing ν and $\kappa \rightarrow j\infty$ at $\nu=1$ for decreasing ν ; for TE $\kappa \rightarrow 0$ at $\nu=1$. Factors $0 \cdot \infty$ and $0/0$ thus appear in equation (A-7), for TE and TM, respectively. They do of course not represent physical reality. It can be shown that Γ is continuous at $\nu=1$, due to the inclusion of κ . – This is shown in Figure A-2, with Γ for a non-resonant TM (Brewster) mode with a load $\varepsilon=52-j20$. ν becomes $|\sqrt{\varepsilon/(\varepsilon+1)}| = 0,992$ ($\sin \theta^i \approx 82,1^\circ$) at the nominal frequency 2450 MHz. κ is set to 0,939 at this frequency. – The system is rather narrow-band, with $\nu=1$ at 2427 MHz and $\nu=1,013$ at 2396 MHz. In the latter case only 28 % of the power is absorbed in the load; the mode energy decay distance d_d (energy density decrease by $\frac{1}{e}$) is then 60 mm. However, the system can of course be matched to $\Gamma=0$ also at this frequency, but then becomes quite narrowband.

In conclusion, using r as the essential property of systems gives incomplete and even misleading results. The coupling impedance ratio κ is indispensable for determination of coupling design and cavity field amplitudes. For microwave heating systems, the coupling factor χ should be close to 1 for system matching. The amplitude and phase of Γ as function of the frequency provide a complete overall picture of the bandwidth and sensitivity of the system, including the expected generator efficiency.

A.4 Simultaneous cavity modes

A.4.1 The equivalent circuit and the TE_x mode amplitude relationships

The equivalent circuit is shown in Figure A-3, for two only cavity modes. – The input line has the characteristic wave impedance Z_g , and the generator has a voltage U . The aperture junction is represented by an ideal transformer and the aperture step capacitance C_a . The mode E fields are thus the same for all modes, apart from the ratios $1:N_1$ and $1:N_2$ which are unequal since the E_n in the Fourier expansion equations for the mode fields of the excitation slot are unequal. The modes are represented as series resonant circuits, with resistances R representing the loss in the load.

The most important conclusion from the equivalent circuit is that *the mode voltage quotients are independent of the total system matching condition*. Of course, the total efficiency of energy transfer will be maximum at matching – but the relative amount of power carried by each mode is independent of that. *The modes are thus orthogonal, irrespective of the aperture data and system matching.*

The impedance transformation is accomplished by the aperture, which makes system matching possible even for highly resonant modes. This is the most important function of the aperture (its second most important function is that it provides some possibilities of mode selection, depending on its length and position). – To the first order and for a narrow slot, the impedance transformation ratio N

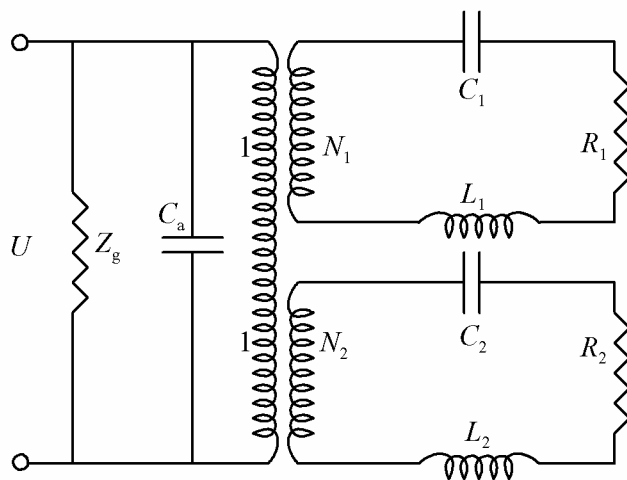


Figure A-3. Equivalent circuit for aperture-coupled cavity with two modes



becomes $\sqrt{c/b}$ [†]. Intuitively, a more narrow slot ($c \rightarrow 0$) becomes better matched to a mode with low field impedance[‡] in the aperture plane, so the formula is reasonable.

The aperture capacitance is typically so small that it does not appreciably influence the situation[§].

A.4.2 Decomposition of TE_x modes into TE_z and TM_z modes

With the load surface in a constant z plane, a pure TE_x mode will no longer propagate as that after traversing the surface. Intuitively, this becomes obvious when the H field there is studied: it has x - and y -directed components and the latter must induce an x -directed current component in the dielectric load. This current is accompanied by a likewise x -directed E component, resulting in a violation of the TE_x mode characteristics.

What happens can be understood by decomposing the $TE_{mn}x$ mode into a $TE_{mn}z$ and a $TM_{mn}z$ mode. For unidirectional propagation, the mode amplitudes C_{TE} and C_{TM} must be such that the condition $E_x=0$ is achieved. Since C for TM modes is for the H field, the factor η_0 in the expression for C_{TM} disappears when the E field is made reference as it is for C_{TE} . Furthermore, $\epsilon=1$ at the excitation. The conditions are thus that $E_{xTMz} + E_{xTEz} = 0$, and $E_{yTMz} + E_{yTEz} = E_{yTEx}$. Using Table A-1 this gives, using the amplitude factors C as reference

$$(A-9) \quad C_{TE_{mn}} = C_{TM_{mn}} \cdot mb/na \cdot \sqrt{1-v^2} \quad (TE_{mn}x \text{ mode})$$

Both wavenumbers m/a and n/b influence the balance between the of TE_z and TM_z components. Equation (A-9) can be intuitively understood by firstly realizing that the H_y and E_x fields of a TM_z mode increase in relation to its overall mode power density when a decreases (m/a increases); therefore an increase of C_{TE} is needed to maintain the E_x field cancellation. Secondly, the H_y and E_x fields of a TE_z mode increase in relation to its overall mode power density when n/b increases; therefore C_{TE} must then decrease. Thirdly, a high v results in weaker horizontal E fields of TM_z modes; they weaken in relation to the overall TM_z mode power density; as a result also the E fields of the TE_z mode must decrease, to maintain the field intensity equality.

Since the $E_{yTEx} = E_n$ mode field amplitudes are what is obtained by the Fourier expansion, the following practical relationships are obtained

$$(A-10) \quad E_{yTM_{mn}} = \frac{E_n \cdot \frac{n^2}{b^2}}{\frac{m^2}{a^2} + \frac{n^2}{b^2}} \quad E_{yTE_{mn}} = -\frac{E_n \cdot \frac{m^2 n^2}{a^2 b^2}}{\frac{m^2}{a^2} + \frac{n^2}{b^2}} = -E_{yTM_{mn}} \cdot \frac{m}{a} \quad E_{yTE_{m0}} = E_0$$

The TE and TM mode propagation in the cavity is always bidirectional, except for TM Brewster modes which are approximately reflectionless. The condition $E_x=0$ in the aperture plane is maintained, which means that the sums (E field differences) ($C_{TE}^+ + C_{TE}^-$) and ($C_{TM}^+ + C_{TM}^-$) must instead be used[§]. It is concluded that the orthogonality between the $TE_{mn}z$ and $TM_{mn}z$ modes is maintained, but their relative amplitudes and phases are determined by the cavity excitation and the reflection factors at the load.

The normalised power absorption in the load of the $TE_{mn}z$ and $TM_{mn}z$ modes becomes orthogonal in terms of the overall power. However, the heating pattern will be determined by the vectorially added fields.

[†] The proof is given in Harrington, section 8-10, p 420-423.

[‡] The mode impedance for TE_x modes is E^+_y/H^+_x and the field impedance is $(E^+_y + E^-_y)/(H^+_x - H^-_x)$.

[§] This is discussed in Harrington, p 418-419, and in Collin (Foundations for Microwave Engineering), p 334.

[§] The plus signs of C_{TE}^- and C_{TM}^- apply when they both refer to the E field. Since the sign for the calculated C_{TM}^- represents the H field, it has to be reversed in some calculations, to provide equality of TEM waves ($v=0$).



A5. Evanescent mode degeneracy

When $\nu > 1$, the orthogonality between the forwards and backwards waves in the cavity airspace disappears. This seems not to be pointed out in the literature, but can readily be shown by considering that the “source” signal C_1^+ is reactive due to the imaginary factor $\sqrt{1-\nu^2}$, and the fact that orthogonality requires a sine or cosine variation which is replaced by exponential decay for evanescent modes; there is thus no phase which is needed for orthogonality.

By taking the Poynting vectors in the usual way one obtains the normalized power[†]:

$$P = \frac{1}{2}\sqrt{1-\nu^2} \cdot (1-|r|^2) \quad (\nu < 1; \text{TM and TE modes; } C^+=1) \quad (\text{A-11a})$$

$$P = \frac{1}{2}\text{Re } S = \frac{1}{2}\text{Re} [(1-r) \cdot \sqrt{1-\nu^2} \cdot (1+r)^*] \quad (\nu > 1; \text{TM mode; } C^+=1) \quad (\text{A-11b})$$

$$P = \frac{1}{2}\text{Re } S = \frac{1}{2}\text{Re} \{ (1+r) \cdot [\sqrt{1-\nu^2} \cdot (1-r)]^* \} \quad (\nu > 1; \text{TE mode; } C^+=1) \quad (\text{A-11c})$$

Note that an imaginary $\sqrt{1-\nu^2}$ is negative.

A6. Load power of aperture-fed cavity TM and TE modes

The TMz modes are treated first. – Since the E_y component is that which determines the the mode amplitudes, the conditions for the E field of this mode is used. The normalisation here is the same as for equation A-11, except that E_{ymn} is now set to 1, for both TEz and TMz modes. The horizontal cross section factors in equation (A-11) are thus not included here.

Firstly, propagating modes are dealt with. Their Poynting vector $\frac{1}{2}\sqrt{1-\nu^2} \cdot (1-|r|^2)$ becomes proportional to the square of the amplitude of the field $(1-r)$, where the cavity r is calculated in the feed plane. Note that r becomes negative for large ν beyond Brewster conditions, since the H field is reference (this applies for the TM modes in this section), so that the factor becomes about 2 near $\nu=1$. Secondly, the input mode E field amplitude is also proportional to $\sqrt{1-\nu^2}$, so that this factor squared must also be included. One obtains the mode power normalised for a input TM mode E field amplitude set to 1 as

$$P_{\text{mode}} = \frac{1}{2} \frac{1-|r|^2}{|1-r|^2 \cdot \sqrt{1-\nu^2}} \quad (\nu < 1; \text{TM mode; } E_{\text{hor}}=1) \quad (\text{A-12a})$$

When $\nu > 1$, the only difference is that the nominator is replaced by the expression in equation (A-11b). Since reduction by $\sqrt{1-\nu^2}$ cannot now be made, one obtains

$$P_{\text{mode}} = \frac{1}{2} \frac{\text{Re}[(1-r)\sqrt{1-\nu^2} \cdot (1+r)^*]}{|1-r|^2 \cdot (\nu^2 - 1)} \quad (\nu > 1; \text{TM mode; } E_{\text{hor}}=1) \quad (\text{A-12b})$$

It is to be noted that P_{mode} represents what is possible to achieve in infinitely many “normalised”[†] cavities having cross section dimensions providing a spectrum of all ν values. The normalisation provides a true comparison for square cavities with mode indices $m=n$, resulting in equal P_{mode} for $\nu=0$.

It is of particular interest what P_{mode} is obtained for $\nu=1$. For TMz modes this is calculated by firstly setting the exponential factors $\exp(\mp jk_0\sqrt{1-\nu^2}z)$ to 1, representing either $z=0$ or $\nu=1$. After insertion in equation (A-12a) above and some manipulations one obtains, with the horizontal E field amplitude 1 again as reference

[†] P is “drastically” normalised in equations A-10 by setting $C^+=1$; $a=b=1$; $m=n=1$; $\lambda_0=1$ and omitting a resulting integration factor. Furthermore, r refers to the E field for TE modes and to the H field for TM modes here and in the following.

$$P_{\text{mode}} = \frac{1}{2} \text{Re}(\varepsilon/\sqrt{\varepsilon-1})$$

($\nu=1$ and ℓ arbitrary; TM mode;
 $E=1$) (A-13)

Pseudo-Brewster TMz modes have $r \approx 0$. In a similar way one then obtains P_{mode} for such modes, under the condition that $r=0$:[‡]

$$P_{\text{mode}} \approx \frac{1}{2} \text{Re}(\varepsilon/\sqrt{\varepsilon-\nu_B^2}) = \frac{1}{2} \text{Re} \sqrt{\varepsilon+1}$$

(TM pseudo-Brewster mode; $E_{\text{hor}}=1$)

(A-14)

Figure A-4 shows the normalised mode amplitudes for two cases of TM modes in a cavity with 110 mm between the ceiling and the infinite dielectric covering the whole cross section at the bottom. The figure shows what should also be expected: that P_{mode} is continuous at $\nu=1$. The requirement is that the cavity feed is by a horizontal slot in the cavity ceiling, providing a constant E mode field = 1 there. The curve in figure A-4 for $\varepsilon=52-j20$ clearly shows that the Brewster mode has the highest amplitude, and there is a distinct inflection point at $\nu=1$; there is also a resonance at $\theta^i \approx 60^\circ$, corresponding to the vertical mode index 1 (λ_g is then about 220 mm).

Brewster modes are non-resonant. Interestingly, resonant TMz modes may exist between these, for $\nu_B < \nu < 1$. Since the load impedance is then *higher* than the wave impedance for the cavity mode, the vertical mode index becomes $\frac{1}{2} + \text{an integer } p \geq 0$. – The $\text{TM}_{\text{mn}\frac{1}{2}}$ mode for $\varepsilon=4-j2$ is also clearly seen as the highest maximum in Figure A-4. There is no $\text{TM}_{\text{mn}1}$ resonance, since this ν value happens to be $\approx \nu_B$.

To avoid the no-load resonance for $\nu=1$, either an index $p=\frac{1}{2}$ mode or an evanescent mode resonance with ν larger than 1 may be employed. Of course, a cavity with a ν giving $p=1$ resonant conditions near the pseudo-Brewster conditions for typical loads is very useful, and a compromise with the $p=\frac{1}{2}$ mode for lower- ε loads may be possible.

For the TEz modes a completely analogous derivation as for the TMz modes gives the following:

$$P_{\text{mode}} = \frac{1}{2} \frac{(1-|r|^2) \cdot \sqrt{1-\nu^2}}{|1+r|^2} \quad (\nu < 1; \text{TE mode; } E=1) \quad (\text{A-15a})$$

$$P_{\text{mode}} = \frac{1}{2} \frac{\text{Re}[(1+r) \cdot \{\sqrt{1-\nu^2} \cdot (1-r)\}^*]}{|1+r|^2} \quad (\nu > 1; \text{TE mode; } E=1) \quad (\text{A-15b})$$

Again, an imaginary $\sqrt{1-\nu^2}$ is negative. – By calculations as for the TM mode one finds that $P_{\text{mode}} \rightarrow 0$ for $\nu \rightarrow 1$. Primary differences to TM modes are that there are no Brewster modes, and that the amplitudes of modes with $\nu \geq 1$ are insignificant. This is shown in figure A-5. – It should again be noted that the real power balance between TEz and TMz modes under conditions of simultaneous excitation as a

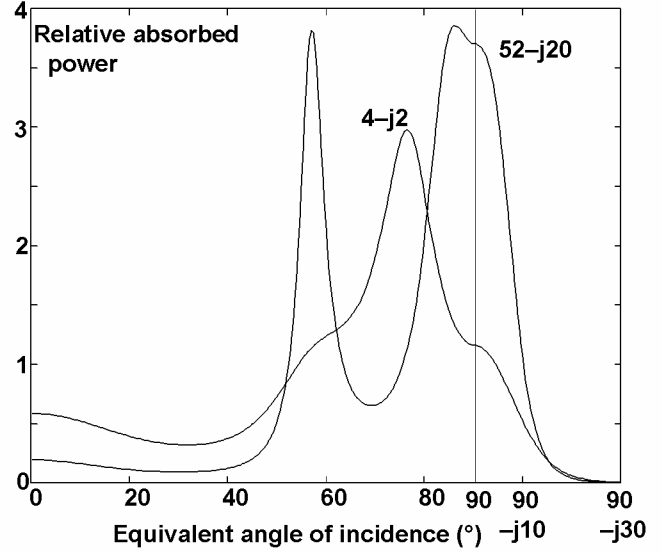


Figure A-4. Relative possible power absorption in loads with 110 mm airspace above

[‡] The pseudo-Brewster condition is calculated by $\nu^2 = |\varepsilon/(\varepsilon+1)|$. – Expanding the general equation in a Taylor series gives also the second order correction. One finds the more accurate formula for the reflected power at θ_B^i : $|r_B|^2 = (\delta/4)^2 \cdot (1-2/|\varepsilon|)$, where δ is in radians. The formula gives a practically insignificant error even for $\tan \delta$ up to 3.

TE_x mode are determined by the horizontal mode indices.

A.7 Mode impedances and coupling

Efficient energy coupling of simultaneous modes requires reasonably similar mode impedances. The power sharing can be deduced by figure A-3, but since only some few if any of the modes are resonant, proper expressions for the absolute value of the impedance of each mode has to be derived.

The field impedance ζ of the mode determines the conditions for system matching. It must then be observed that only that part of the H field which is in time phase with the E field couples power to the load and can provide impedance matching. One obtains

$$\text{Re } \zeta = \frac{E}{H \cdot \cos \phi} = \frac{|\sqrt{1-v^2} \cdot (1-r)|}{|1+r| \cdot \cos \phi} \quad [\cos \phi = \text{atan}(\text{Re } E; \text{Im } E) - \text{atan}(\text{Re } H; \text{Im } H)] \quad (\text{A-16})$$

The equation is valid for all v . – Of course, one may also calculate the absolute value of ζ , to obtain an idea of the overall mode impedance. It may, however, then be better to instead calculate $\text{Im } \zeta$.

Interestingly, the absolute value of ζ passes “horizontally” through the point $v=1$ at a value which gives an almost constant and lower $|\zeta|$ than $\text{Re } \zeta$. This $|\zeta|$ is also essentially ε -independent, from about $|\varepsilon|=4$ to 60. Only if the distance ℓ is small does $\text{Im } \zeta$ disappear.

As for P_{mode} , the $\text{Re } \zeta$ value for $v=0$ is obtained in a simple form:

$$\text{Re } \zeta = \frac{\sqrt{\varepsilon-1}}{\varepsilon} \quad (v=1; \text{TM}) \quad (\text{A-17})$$

Figure A-6 shows the features of $\text{Re } \zeta$ for TM modes in a 183 mm high cavity with a 3 mm thick load.

There are three important features of $\text{Re } \zeta = f(v)$:

- it becomes so high for anti-resonant conditions that power coupling to the load becomes virtually impossible

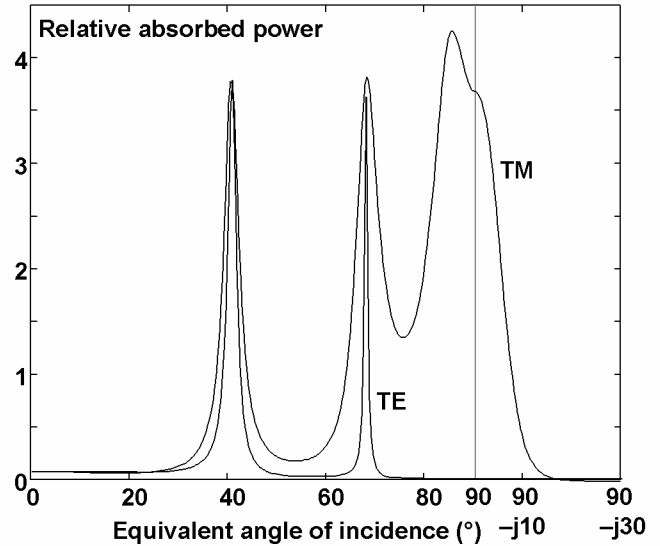


Figure A-5. Relative possible power absorption in a load with permittivity 52–j20; 160 mm airspace above

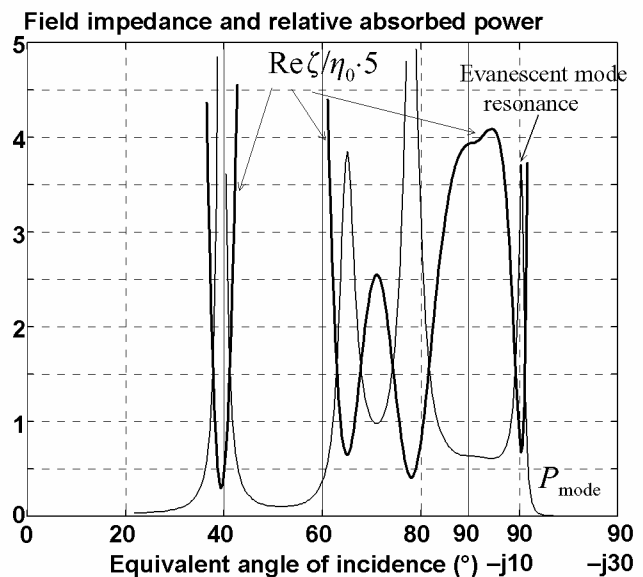


Figure A-6. Field impedance (real) and relative possible power absorption in a 3 mm thick load with permittivity 52–j20; 160 mm airspace above and 20 mm below.



- it becomes low and about of the same value ($0,1\eta_0$ to $0,2\eta_0$) for low- ν resonances
- it becomes very high for $\nu \gg 1$, thus not “disturbing” the situation for power-propagating modes.

Of particular interest is that the impedance remains reasonably the same over a fairly large θ interval: from 80° to $(90-j5)^\circ$ (corresponding to $0,985 < \nu < 1,004$). This means that there are no complicated matching problems between the transmission line and the cavity when such modes are employed alone or together with other (resonant) modes.

The final conclusion in this section is that Brewster modes and modes with ν approaching 1 may indeed play a much larger role in microwave ovens than commonly believed. They offer a series of advantages which must in reality be utilized in many ovens designs, intentionally or unintentionally. The knowledge provided here may become a tool for proper application of these modes, while avoiding the problems associated with cavity wall losses in empty operation.

APPENDIX Field amplitudes and characteristic mode impedances

The horizontal variations are sine and cosine functions in $m\pi x/a$ and $n\pi y/b$ and are given in the table as for example $\mathbf{c}_m \cdot \mathbf{s}_n$, where \mathbf{c}_m is $\cos(m\pi x/a)$ and \mathbf{s}_n is $\sin(n\pi y/b)$. There are amplitude constants C^\pm of the $\pm z$ -directed waves. The propagation factors $\exp(\mp jk_z z)$ are multiplied by C^\pm . These terms are marked by ζ^+ and ζ^- in the table, respectively. Index i on ζ and ε is also omitted. $\varepsilon = 1$ in the empty cavity space. The C factors are for E (TEz) and for H (TMz, TEy), respectively.

Field quantity	TEz mode	TMz mode	TEy mode [†]
H_x	$+(\zeta^+ - \zeta^-) \cdot m \sqrt{\varepsilon - \nu^2} / (a \eta_0) \cdot \mathbf{s}_m \cdot \mathbf{c}_n$	$+(\zeta^+ + \zeta^-) \cdot n / b \cdot \mathbf{s}_m \cdot \mathbf{c}_n$	$+(\zeta^+ + \zeta^-) \cdot j m n \lambda_0 / (2 a b \eta_0) \cdot \mathbf{s}_m \cdot \mathbf{c}_n$
H_y	$+(\zeta^+ - \zeta^-) \cdot n \sqrt{\varepsilon - \nu^2} / (b \eta_0) \cdot \mathbf{c}_m \cdot \mathbf{s}_n$	$-(\zeta^+ + \zeta^-) \cdot m / a \cdot \mathbf{c}_m \cdot \mathbf{s}_n$	$-(\zeta^+ + \zeta^-) \cdot 2 j [\varepsilon - (n \lambda_0 / 2 b)^2] / (\lambda_0 \eta_0) \cdot \mathbf{c}_m \cdot \mathbf{s}_n$
H_z	$-(\zeta^+ + \zeta^-) \cdot 2 j \nu^2 / (\lambda_0 \eta_0) \cdot \mathbf{c}_m \cdot \mathbf{c}_n$	0	$-(\zeta^+ - \zeta^-) \cdot n \cdot \sqrt{\varepsilon - \nu^2} / (b \eta_0) \cdot \mathbf{c}_m \cdot \mathbf{c}_n$
E_x	$+(\zeta^+ + \zeta^-) \cdot n / b \cdot \mathbf{c}_m \cdot \mathbf{s}_n$	$-(\zeta^+ - \zeta^-) \cdot m \eta_0 \sqrt{\varepsilon - \nu^2} / (a \varepsilon) \cdot \mathbf{c}_m \cdot \mathbf{s}_n$	$-(\zeta^+ - \zeta^-) \cdot 2 j \sqrt{\varepsilon - \nu^2} / \lambda_0 \cdot \mathbf{c}_m \cdot \mathbf{s}_n$
E_y	$-(\zeta^+ + \zeta^-) \cdot m / a \cdot \mathbf{s}_m \cdot \mathbf{c}_n$	$-(\zeta^+ - \zeta^-) \cdot n \eta_0 \sqrt{\varepsilon - \nu^2} / (b \varepsilon) \cdot \mathbf{s}_m \cdot \mathbf{c}_n$	0
E_z	0	$-(\zeta^+ + \zeta^-) \cdot 2 j \nu^2 \eta_0 / (\lambda_0 \varepsilon) \cdot \mathbf{s}_m \cdot \mathbf{s}_n$	$+(\zeta^+ + \zeta^-) \cdot m / a \cdot \mathbf{s}_m \cdot \mathbf{s}_n$
η_g	$\eta_0 / \sqrt{\varepsilon - \nu^2}$	$\eta_0 \cdot \sqrt{\varepsilon - \nu^2} / \varepsilon$	$\eta_0 \cdot \sqrt{\varepsilon - \nu^2} / [\varepsilon - (n \lambda_0 / 2 b)^2]$
S_z^+	$2 C^+ ^2 \cdot \text{Re}(\sqrt{\varepsilon - \nu^2}) \cdot \nu^2 a b / (\eta_0 \lambda_0^2)$	$2 C^+ ^2 \cdot \text{Re}(\sqrt{\varepsilon - \nu^2} / \varepsilon) \cdot \eta_0 \nu^2 a b / \lambda_0^2$	$2 C^+ ^2 \cdot \text{Re}[\sqrt{\varepsilon - \nu^2} / (\varepsilon - (n \lambda_0 / 2 b)^2)] \cdot a b / (\eta_0 \lambda_0^2)$
$P_{\text{wall}} / S_z^{\ddagger}$	$4 R_s / \eta_0 a b \cdot [\nu^2 (a+b) / \sqrt{1 - \nu^2} + \lambda_0^2 \cdot \sqrt{1 - \nu^2} / (4 \nu^2) \cdot (m^2 / a + n^2 / b)]$	$R_s \cdot (m^2 / a^3 + n^2 / b^3) \cdot \lambda_0^2 / (\eta_0 \nu^2 \cdot \sqrt{1 - \nu^2})$	—
$P_{\text{end}} / S_z^{\S}$	$R_s \sqrt{1 - \nu^2} / \eta_0$	$R_s / (\eta_0 \cdot \sqrt{1 - \nu^2})$	—

[†] The formulas for the impedance and Poynting vectors for these modes are the first order, and given by E_x and H_y only. The theory for hybrid modes is rather involved, since the excitation properties must normally be included. The formulas in the table are for the simplified case of equal “nulling” amplitudes of the TEz and TMz modes, and no change of the balance between these upon reflection.

[‡] The side walls of the waveguide, with equal surface resistance R_s (Ω/\square).

[§] The end wall of the waveguide, with surface resistance R_s (Ω/\square).